Available online at www.sciencedirect.com

ScienceDirect

Advances in Space Research 75 (2025) 1653–1664

ADVANCES IN SPACE RESEARCH (a COSPAR publication)

www.elsevier.com/locate/asr

# Quantum gravimetry for future satellite gradiometry

Mohsen Romeshkani [a,*], Jürgen Müller [a], Annike Knabe [a], Manuel Schilling [b]

[a] Leibniz University Hannover, Institute of Geodesy, Schneiderberg 50, Hannover 30167, Germany
[b] German Aerospace Center (DLR), Institute for Satellite Geodesy and Inertial Sensing, Callinstraße 30B, Hannover 30167, Germany

Received 18 May 2024; received in revised form 25 November 2024; accepted 27 November 2024
Available online 3 December 2024

**Abstract**

The present electrostatic accelerometers (EA) drift at low frequencies. To address this problem, integrating a cold atom interferometry (CAI) accelerometer could be beneficial, as it offers the potential for superior long-term stability. The CAI-based accelerometers (CAI ACC) are accurate and stable, but they have some issues with long dead times and a relatively small dynamic range. A way to address these problems is to combine a CAI ACC with an EA in a hybrid configuration. Using CAI ACC in an upcoming satellite gradiometry mission can give stable and accurate measurements of the static Earth's gravity field. Three scenarios have been considered in this study: first, a realistic scenario involving current-generation and realistic hybrid accelerometers; second, a semi-realistic scenario with the same accelerometers and an accurate gyroscope; and third, using highly accurate hybrid/CAI accelerometers with an optimistic gyroscope. One significant aspect was on detecting temporal gravity changes, which cannot compare to the effectiveness of the low-low satellite-to-satellite tracking (LLSST) principle. But, quantum gradiometers can significantly enhance solutions for the static gravity field, provided one has accurate observations of the satellite orientation available.


*Keywords:* Earth's gravity field; Quantum accelerometer; Cold atom interferometer (CAI); Satellite gravity gradiometry (SGG); Hybrid accelerometer; Next generation gravity mission

## 1. Introduction

Specialized satellite gravimetry missions like GOCE (Gravity Field and steady-state Ocean Circulation Explorer) (Drinkwater et al., 2003), GRACE (Gravity Recovery and Climate Experiment) and GRACE-FO (Tapley et al., 2004; Flechtner et al., 2017; Kornfeld et al., 2019) offer distinctive datasets regarding the static and time variable gravity field of the Earth across different spatiotemporal scales. Nevertheless, in light of the remarkable results from these missions, a ubiquitous constraint emerged at the instrument level. One of the limiting factors is the noise behavior of the EA used in these satellite gravimetry missions. Accelerometers are important tools for studying gravity from space. They help distinguish gravitational forces from other forces like atmospheric drag and solar radiation pressure.

Current satellite missions employ EAs, known for their minimal noise levels at medium–high frequencies. Nevertheless, these accelerometers exhibit certain limitations, including low-frequency drift and challenges in accurately estimating time variable biases and scale factors. To mitigate the limitations of EAs, multiple innovative concepts and novel technologies have been introduced.

The CAI offers a promising solution to these challenges. CAI employs a cloud of independent cold atoms as the test mass within an atom interferometer. The key advantage of atom interferometry accelerometers lies in their remarkable long-term stability and the precise scale factor determination, which relies on the frequency stability of the laser system.

* Corresponding author.
*E-mail address:* romeshkani@ife.uni-hannover.de (M. Romeshkani).

https://doi.org/10.1016/j.asr.2024.11.072
0273-1177/

In the context of CAI accelerometery, the determination of an unknown acceleration is achieved by analysing the phase shift between two interfering atomic states within an atom cloud. This phase shift occurs subsequent to the manipulation of the atom cloud using pulses from two counter-propagating laser beams (Meister et al., 2022; Lévèque et al., 2022; Antoine and Bordé, 2003). Simulation studies, exemplified by the works of Abrykosov et al. (2019), Migliaccio et al. (2023) and Müller and Wu (2020), demonstrate substantial potential enhancements in gravity field recovery through the utilization of CAI.

Nonetheless, employing a standalone CAI ACC as an instrument carries inherent limitations, primarily associated with extended interrogation times during which transient short-term non-gravitational or gravitational forces remain unobservable. A potential solution to this issue involves the concept of hybridization, where the idea is to integrate an EA, renowned for its high-frequency domain measurement capabilities, with the highly precise CAI ACC providing long-term stability. Such a hybrid sensor represents a fusion of a CAI ACC and an EA. This approach has been explored in a few studies (e.g. Zahzam et al., 2022), which investigate hybrid sensors and various methods of hybridization.

Douch et al. (2018) investigates the performance of a CAI gradiometer for satellite gravity field measurements. Through closed-loop numerical simulations, the study shows that a CAI gradiometer, particularly in the quasi-inertial mode, can significantly outperform missions like GOCE, provided it meets stringent technical requirements. The study concludes that such a CAI gradiometer mission could offer improved precision in gravity field recovery, highlighting the potential of this technology for future satellite missions.

The recently initiated CARIOQA-PMP (Cold Atom Rubidium Interferometer in Orbit for Quantum Accelerometery – Pathfinder Mission Preparation; funded by the European Union[1]) has set its sights on elevating the Technology Readiness Level and laying the groundwork for a Quantum Pathfinder Mission in space gravimetry by the year 2030 (Lévèque et al., 2022). The aim of CARIOQA-PMP is to develop an engineering model of a quantum accelerometer, advancing key technologies, and conducting a scientific study to explore the potential applications of quantum sensors for determining Earth's gravity field from space. Additionally, the project seeks to define the corresponding requirements for the sensor technology and for an improved future satellite mission. The study examines the various scenarios of a pure quantum gravimetry mission or a mission that uses quantum and classical sensors in a hybrid manner.

The focus of study is on using CAI technology in a satellite gradiometry mission. The study first identifies suitable quantum sensors for observing the Earth's gravitational field and describes the corresponding error characteristics. To accomplish this, the paper is organized in the following manner: The properties of EA and CAI ACC are presented in the second section. The third section is related to the closed-loop simulation. The results of simulation studies are summarized in the fourth section. Eventually, the main conclusions of this study are provided in the fifth section.

## 2. Performance of sensors

### 2.1. Electrostatic accelerometers

In current satellite gravimetry missions, a challenge arises due to the drift of the EA, contributing notable errors, especially at lower frequencies (Christophe et al., 2015; Kupriyanov et al., 2024). In this study, we focus on two EAs that are more accurate and high technology included. One of them pertains to the encouraging outcomes achieved by the LISA Pathfinder (LPF) mission (Armano et al., 2018). The favourable results obtained from the Gravitational Reference Sensor (GRS) during the LISA-Pathfinder mission have stimulated several investigations assessing the performance of a simplified Gravitational Reference Sensor (SGRS) for low Earth orbits (Dávila Álvarez et al., 2022). Unlike EAs, which detect the displacement of the test mass (TM) using capacitance and apply electrostatic force, optical accelerometers track the test mass by utilizing laser interferometry. Another EA is related to the the French aerospace lab ONERA (Dalin et al., 2020) that designed and built the accelerometers for satellite missions GRACE, GOCE and GRACE-FO.

#### 2.1.1. SGRS (simplified gravitational reference sensor)

The EA of GRACE-FO, the current satellite gravimetry mission, is a significant error source in the measurement process. Previous studies (e.g. Purkhauser and Pail, 2020) have demonstrated its insufficiency for multi-pair satellite configurations at lower altitudes, thereby constraining the accuracy of the Earth's gravity field recovery.

SGRS (Dávila Álvarez et al., 2022) presents a technological approach to enhance the measurement of non-gravitational accelerations in GRACE-like missions and differential gravitational accelerations in GOCE-like missions to a satisfactory level suitable for satellite gravimetry. The design of the SGRS is a follow up of promising performance of the LPF (GRS), which acts as a precision inertial sensor (Dolesi et al., 2003; Armano et al., 2018). The SGRS, being a scaled-down version of the LPF GRS, features reduced mass and complexity while being optimized for enhanced performance in upcoming satellite gravimetry missions (Dávila Álvarez et al., 2022).

Regarding to the most important forces in satellite gravimetry missions, a model for acceleration noise in the SGRS has been formulated, considering two operational scenarios: non-drag-compensated at an orbit altitude of 500 km (comparable to GRACE and GRACE-FO):

[1] https://doi.org/10.3030/101081775.

$$S^{\frac{1}{2}}(f) = 10^{-10}\ \mathrm{ms}^{-2}\ \mathrm{Hz}^{-\frac{1}{2}} \times \left[3 \times 10^{2}\left(\frac{f}{1\mathrm{Hz}}\right)^{2} + 5 \times 10^{-3} \times \left(1 + \frac{1\mathrm{Hz}}{f}\right)^{\frac{1}{3}}\right] \quad (1)$$

and drag-compensated for an altitude of 350 km:

$$S^{\frac{1}{2}}(f) = 10^{-10}\ \mathrm{ms}^{-2}\ \mathrm{Hz}^{-\frac{1}{2}} \times \left[3 \times 10^{2}\left(\frac{f}{1\mathrm{Hz}}\right)^{2} + 4 \times 10^{-3} \times \left(1 + \frac{700\mu\mathrm{Hz}}{f} + \left(\frac{300\mu\mathrm{Hz}}{f}\right)^{2}\right)^{\frac{1}{2}}\right]. \quad (2)$$

These scenarios represent the optimal realistic operational conditions concerning gravity recovery sensitivity (Dávila Álvarez et al., 2022).

Expected to perform better than the GRACE-FO accelerometers when arranged in a polar pair configuration, the SGRS shows promising potential for reducing acceleration noise. If the sensor would be operated on a drag-compensated platform (which is considered here in our gradiometry concept/scenario), its performance would further improve (Dávila Álvarez et al., 2022). For better understanding of the significance of the SGRS, we compare it with the LISA-based accelerometer (Armano et al., 2018):

$$S^{\frac{1}{2}}(f) = 10^{-10}\ \mathrm{ms}^{-2}\ \mathrm{Hz}^{-\frac{1}{2}} \times \left[3 \times 10^{-2} + \frac{30f}{1\mathrm{Hz}}\right] \quad (3)$$

Fig. 1 shows a comparison of the amplitude spectral density (ASD) of the aforementioned accelerometers. The effect of the drag-free system is obvious in comparison of the SGRS EA with and without drag-free system. Most of this effect is concentrated at the low-frequency part. Another important point is related to the capacitive sensing contribution noise in SGRS accelerometers. The effect of this source noise appears in the high frequency part (Josselin et al., 1999; Dávila Álvarez et al., 2022).

### 2.1.2. H-STAR

The most accurate accelerometers for space applications currently available are the EA developed by the French aerospace lab ONERA. These accelerometers possess the capability to measure spacecraft non-gravitational acceleration to approximately $10^{-11}\frac{m}{s^2/\sqrt{Hz}}$ within the frequency range of about 1 mHz–1 Hz (Touboul et al., 2016).

One of the EA under investigation in this research, referred to as the H-STAR accelerometer, is ingeniously engineered, featuring a disruptive mechanical design that permits the use of a compact 30 × 30 × 30 $\mathrm{mm}^3$ proof-mass while maintaining an exceptional performance across all three axes. Dalin et al. (2020) introduced this new EA accelerometer with the following ASD:

$$S^{\frac{1}{2}}(f) = 10^{-11}\ \mathrm{ms}^{-2}\ \mathrm{Hz}^{-\frac{1}{2}} \times \left[2.4 \times 10^{-2}\left(\frac{1\mathrm{Hz}}{f}\right)^{0.25} + 1 \times 10^{-7}\left(\frac{1\mathrm{Hz}}{f}\right)^{2} + 8 \times \frac{f^{2}}{1\mathrm{Hz}}\right]. \quad (4)$$

Fig. 1 shows the error behaviour of this accelerometer. This H-STAR accelerometer has a drift in low frequencies and an excellent performance is in the high frequency part.

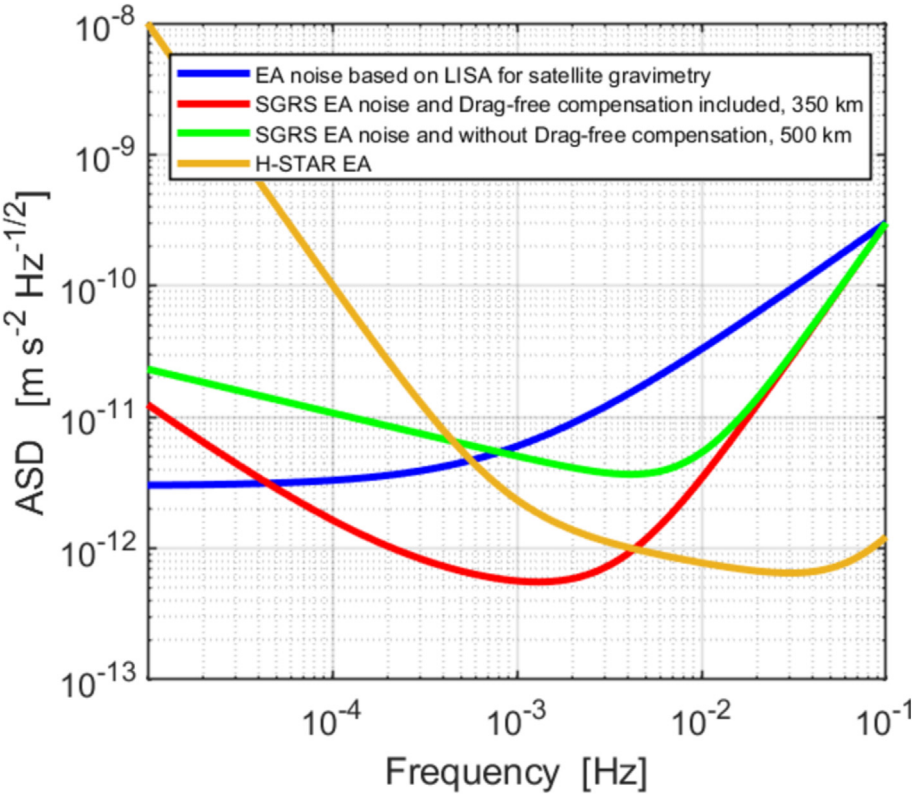


Fig. 1. Amplitude spectral densities (ASDs) in terms of acceleration noise for different classical EA and LISA.

The error ASD is the summation of different error sources for this accelerometer. Fig. 1 shows the H-STAR EA has the best performance in high frequency part compared to the SGRS ACCs, and a weaker performance in the low frequency part.

### 2.2. CAI accelerometers

The CAI employs atom clouds as test masses within an interferometer, implemented through a series of three precise laser pulses which serve as both beam splitters and mirrors. Laser pulses, administered with a time interval denoted as $T$, are employed to separate and to reunite the atoms, inducing distinct momentum states in accordance with the superposition principle (Pereira dos Santos and Landragin, 2007; Schilling et al., 2012).

The error behavior of a CAI ACC depends on different parameters (Meister et al., 2022; Knabe et al., 2022; Lévèque et al., 2022) but here we focus on two different white noise levels of CAI ACC. A CAI ACC with noise level of $10^{-11}\frac{m}{s^2/\sqrt{Hz}}$ (CAI 11) represents a state-of-the-art device (i.e. a theoretical device based on current technology in terrestrial gravimetry or laboratory experiments) in the following called "realistic CAI ACC". We can also consider a CAI ACC with noise level of $10^{-12}\frac{m}{s^2/\sqrt{Hz}}$ (CAI 12) as a "future CAI ACC".

### 2.3. Hybrid accelerometers

The EA exhibits established short-term sensitivity and a demonstrated flight heritage, while CAI ACC offers time-invariant measurement stability and absolute measurements, making calibration processes unnecessary. These technologies appear highly complementary, and a hybrid accelerometer combining their strengths presents novel opportunities for space-based inertial measurements. The chosen way for simulating a hybrid Accelerometer (ACC) is the combination in the frequency domain.

#### 2.3.1. Hybrid accelerometers with CAI 11

Fig. 2 illustrates the hybridization of EAs and the actual CAI 11, which is the realistic CAI ACC.

In delineating our methodology, the determination of a cut-off frequency assumes significance, defining the proportional contributions of EA and CAI ACC in the hybrid ACC. Optimal cut-off frequency selection involves considering the intersection of the ASD of EA and CAI ACC. In Fig. 2(a), the combination of H-STAR and CAI 11 is illustrated, showcasing the elimination of H-STAR drift through hybridization. An additional advantage is given in the high-frequency domain, leveraging the high-accuracy characteristics of H-STAR. The contributions of H-STAR and CAI 11 are nearly equal in this hybridization. In Fig. 2(b), the fusion of a SGRS EA and CAI 11 is depicted. As discussed in Section 2.1.1, SGRS encompasses a capacitive sensing error in the very high-frequency range, distinguishable from the H-STAR EA. Unlike the prior hybridization, the low-frequency behaviour of SGRS is deemed suitable, while the high-frequency segment poses a challenge. In this scenario, we endeavour to integrate SGRS in the high-frequency domain using CAI 11. Dual cut-off frequencies are used—one in the low-frequency range (with minimal impact) and another in the high-frequency range, mitigating the capacitive sensing error of SGRS. Notably, the contribution of SGRS surpasses that of CAI 11 in the final hybrid configuration.

#### 2.3.2. Hybrid accelerometers with CAI 12

Here, we look at the future hybridization by using CAI 12.

Fig. 3(a) shows the combination of H-STAR and CAI 12 with one cut-off frequency. This hybridization decreases the contribution of H-STAR with respect to the CAI 12 and indeed the H-STAR does not have any significant contribution with respect to the CAI 12 only here.

Fig. 3(b) shows the combination of SGRS and CAI 12. Similar to the realistic hybridization, we use two cut-off frequencies. The SGRS contribution is now reduced in the low and high frequency parts. The only relevant contribution of SGRS in this hybridization is the medium frequency part.

### 2.4. Gyroscopes

The GOCE mission was capable of measuring both diagonal and non-diagonal components through a three-dimensional gradiometer. Given the presence of non-diagonal components in the GOCE observations, it is possible to reconstruct and enhance the attitude data, as demonstrated by Siemes (2018). Considering the operational intricacies of CAI ACC, we assume having a single sensitive axis in the first space realisation. In our study, we exclusively utilize the diagonal components of the gradiometry tensor. This then requires an alternative approach to measure the gradiometer attitude and the angular velocities (Stummer et al., 2011; Siemes, 2018). In this context, we examine two distinct gyroscopes characterized by varying noise levels. The first one has a white-noise level of $10^{-8}\frac{rad}{s/\sqrt{Hz}}$ that this is for a fibre optic gyroscope, ASTRIX200[2] in terms of angular velocity that we call realistic gyroscope (R Gyro). The other one is a CAI-based gyroscope and has different noise levels depending on the interrogation time of the atoms in the interferometry. This represents the future gyroscope with a white-noise level close to $10^{-9}\frac{rad}{s/\sqrt{Hz}}$ (Savoie et al., 2018).

### 2.5. Gradiometer

In space gravimetry missions, a gradiometer setup typically involves placing two or more accelerometers inside a

[2] https://www.airbus.com/.

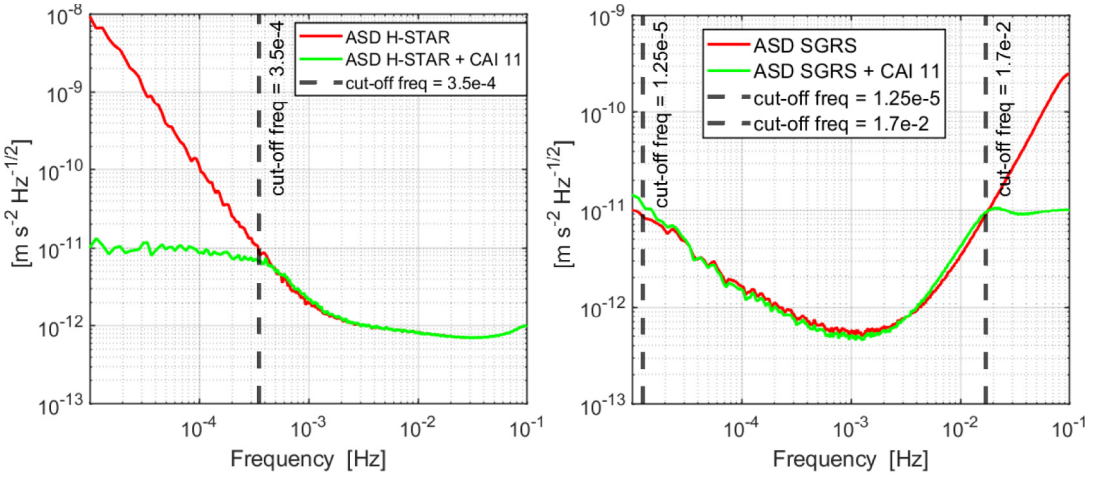


(a) (b)

Fig. 2. ASD of hybrid accelerometer noise, H-STAR + CAI 11 (a) and SGRS + CAI 11 (b).

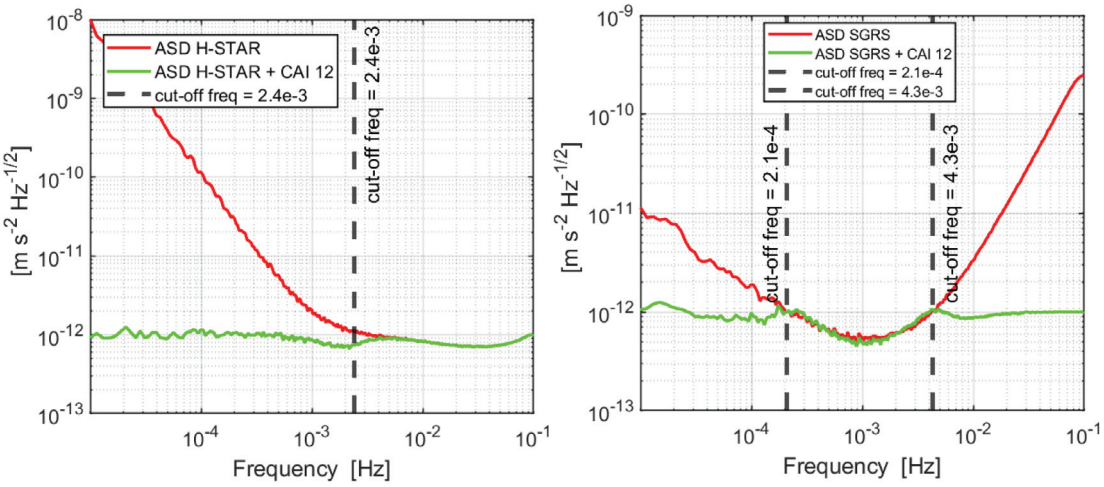


(a) (b)

Fig. 3. ASD of hybrid accelerometers, H-STAR + CAI 12 (a) and SGRS + CAI 12 (b).

spacecraft. These accelerometers are positioned to measure the varying differential accelerations between them along different directions. For instance, in the GOCE mission, the gradiometer comprised three pairs of accelerometers set up orthogonally. Each pair had two accelerometers aligned along the same axis. This setup enables the gradiometer to measure changes in gravitational acceleration along three perpendicular axes at the same time.

In our study, we use a gradiometer setup similar to the one used in GOCE, keeping the same distance and configuration between the accelerometers, but replacing the electrostatic accelerometer (EA) with a hybrid accelerometer. The major difference is the use of 1D accelerometers in our gradiometer. The positioning of the CAI ACC relative to the EA plays a crucial role in determining the achievable sensitivity for the hybrid ACC. The CAI ACC can be placed in front of the EA along the along-track axis, on top of the EA along the radial axis, or next to the EA along the cross-track axis of the satellite. According to HosseiniArani et al. (2024), the last configuration has significant advantages over the other two possible placements for SST missions, as then the big angular velocity about the cross-track axis in Earth-pointing mode has a largely reduced effect. However, in a gradiometry constellation, the placement of the CAI ACC relative to the EA has been determined based on the direction of the desired sensitivity axis. Fig. 4 illustrates the gradiometer and the hybrid ACCs as a cube. Regarding to the sensitivity axis of the hybrid ACCs, we focus on the diagonal components of the Marussi tensor (Zund, 1994; Torge and Müller, 2023) due to operational constraints of the selected accelerometers.

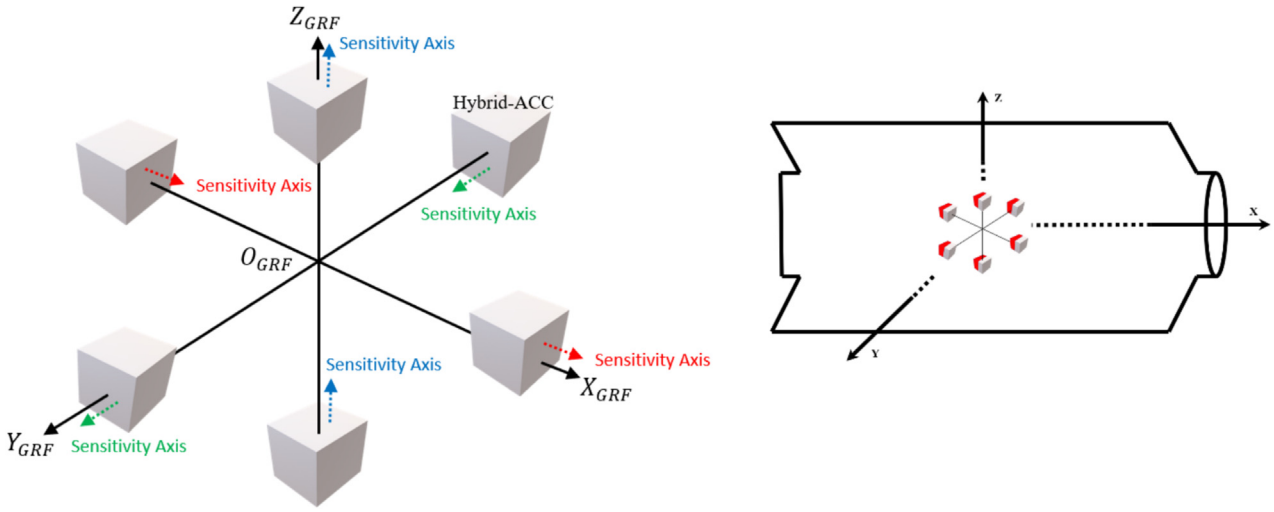


Fig. 4. 3D gradiometer formed by the combination of 1D hybrid accelerometers.

## 3. Closed-loop simulation

Our simulations spanned two months, with data collected at 5-second sampling rate. Although a polar orbit is considered the best for recovering gravity fields from satellite missions, we opted for a GOCE-like orbit with a 96.7° inclination and 250 km altitude to make a fair comparison with GOCE, the reference for gradiometry. Fig. 5 illustrates the flowchart of forward and backward modeling through closed-loop simulations.

For forward modeling and in order to simulate the true world, we used the GOCO05s model as the reference for Earth's gravity field. To consider time variability, We introduced non-tidal time-variable gravity components (i.e., AOHIS components from the ESA Earth System Model, ESM, Dobslaw et al., 2015) and excluded tidal components in this analysis. Both static and time-variable components of the gravity field were expanded up to the spherical harmonic degree/order of 180 in this study. Instrument noise, gradiometer noise (ΔSGG), and attitude noise (ΔATT) are introduced in the simulation process, affecting the accuracy and precision of the collected gradiometry data. These noise sources are combined to produce the noisy data (NSGG), which represents the actual data obtained from the satellite under real-world conditions.

In backward modeling, we employed a common least-squares (LS) adjustment approach to recover the gravity field. This involved using a static spherical-harmonic parametrization. Due to the vast number of observations and numerous unknowns, creating and inverting the normal matrix pose significant numerical challenges. The unknown parameters were determined by inverting the normal matrix, commonly known as the "brute-force" approach (Roth et al., 2012), which also provides information about variances and covariances of the estimated parameters. The maximum spherical harmonic degree in the normal equations matches that of the simulated data. Therefore, in the presented simulation results the impact of possible spectral leakage is not taken into account.

## 4. Mission scenarios and simulation results

Taking into account the different noise levels of CAI ACCs and the utilization of various gyroscopes in the gradiometry concept, we defined three categories: realistic, semi-realistic and future.

### *4.1. Realistic category (Realistic hybrid ACCs and Realistic Gyro)*

The first group involves hybrid accelerometers that combine EAs (SGRS and H-STAR) with CAI 11. This category uses a realistic gyroscope and a realistic hybrid ACC. It includes: (a) SGRS + CAI 11 + Realistic Gyro, (b) H-STAR + CAI 11 + Realistic Gyro, and (c) CAI 11 only + Realistic Gyro. Fig. 6(a) shows the comparable view of these cases on degree variances.

### *4.2. Semi-realistic category (Realistic hybrid ACCs and Future Gyro)*

The second group combines a realistic hybrid accelerometer with a future gyroscope. The realistic hybrid ACC merges EAs with CAI 11. Due to the expected lower noise of this CAI-based gyroscope, we call this category the semi-realistic category. It consists of: (a) SGRS + CAI 11 + CAI Gyro, (b) H-STAR + CAI 11 + CAI Gyro, and (c) CAI 11 only + CAI Gyro. The only difference between this category and the realistic category is the type of gyroscope used.

Fig. 6(b) shows the difference in the simulation results between the cases of this category and highlights the advantage of having EAs compared to the scenario with

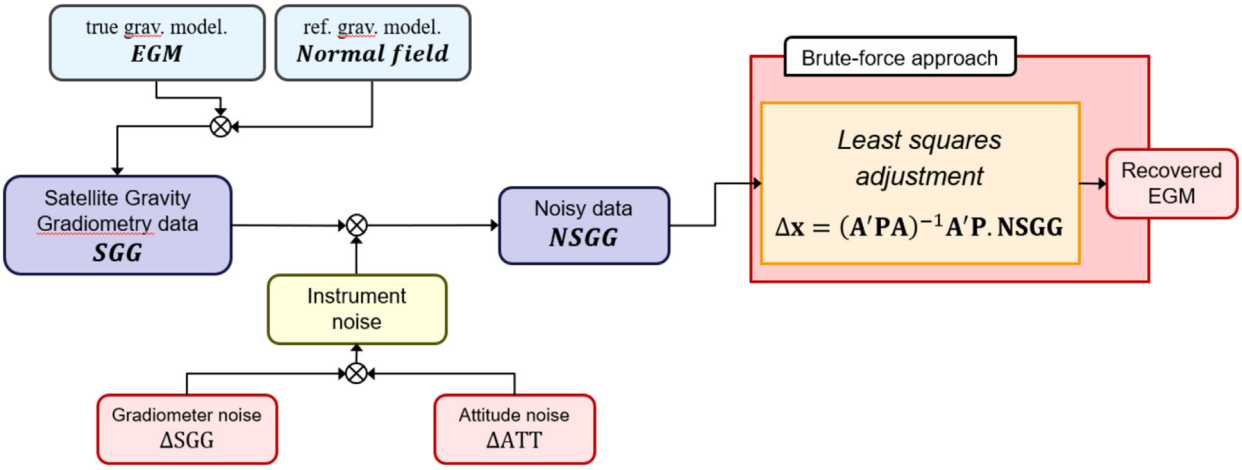


Fig. 5. Flowchart of closed-loop simulation in the gradiometry concept.

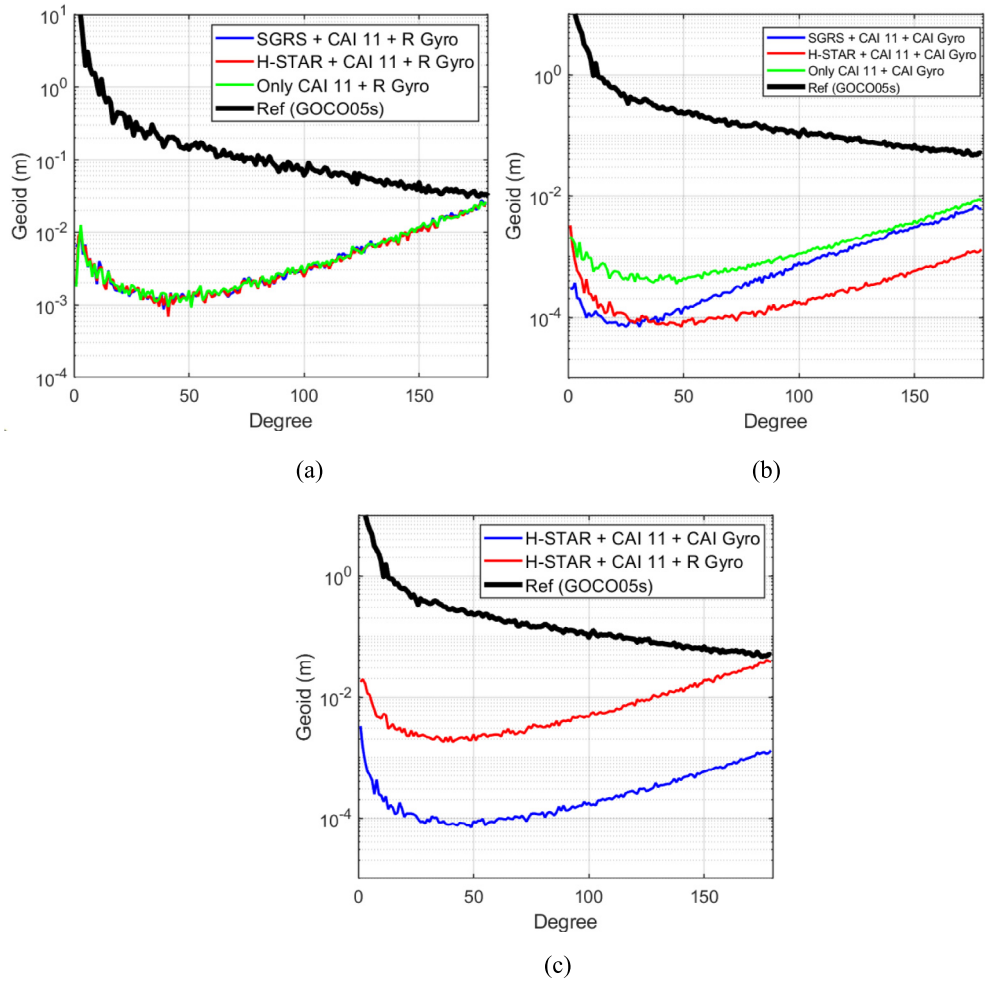


Fig. 6. Performance of the gradiometry concept in the realistic category (a), in the semi-realistic category (b) and with the use of an accurate gyroscope (c).

CAI only. When comparing the realistic and semi-realistic categories, the advantage of having an accurate gyroscope becomes evident in comparison with using a realistic gyroscope. This advantage is shown in Fig. 6(c), which compares two combinations: "H-STAR + CAI 11 + CAI Gyro" and "H-STAR + CAI 11 + R Gyro." A minimum one-order improvement is obtained, particularly at higher degree/order.

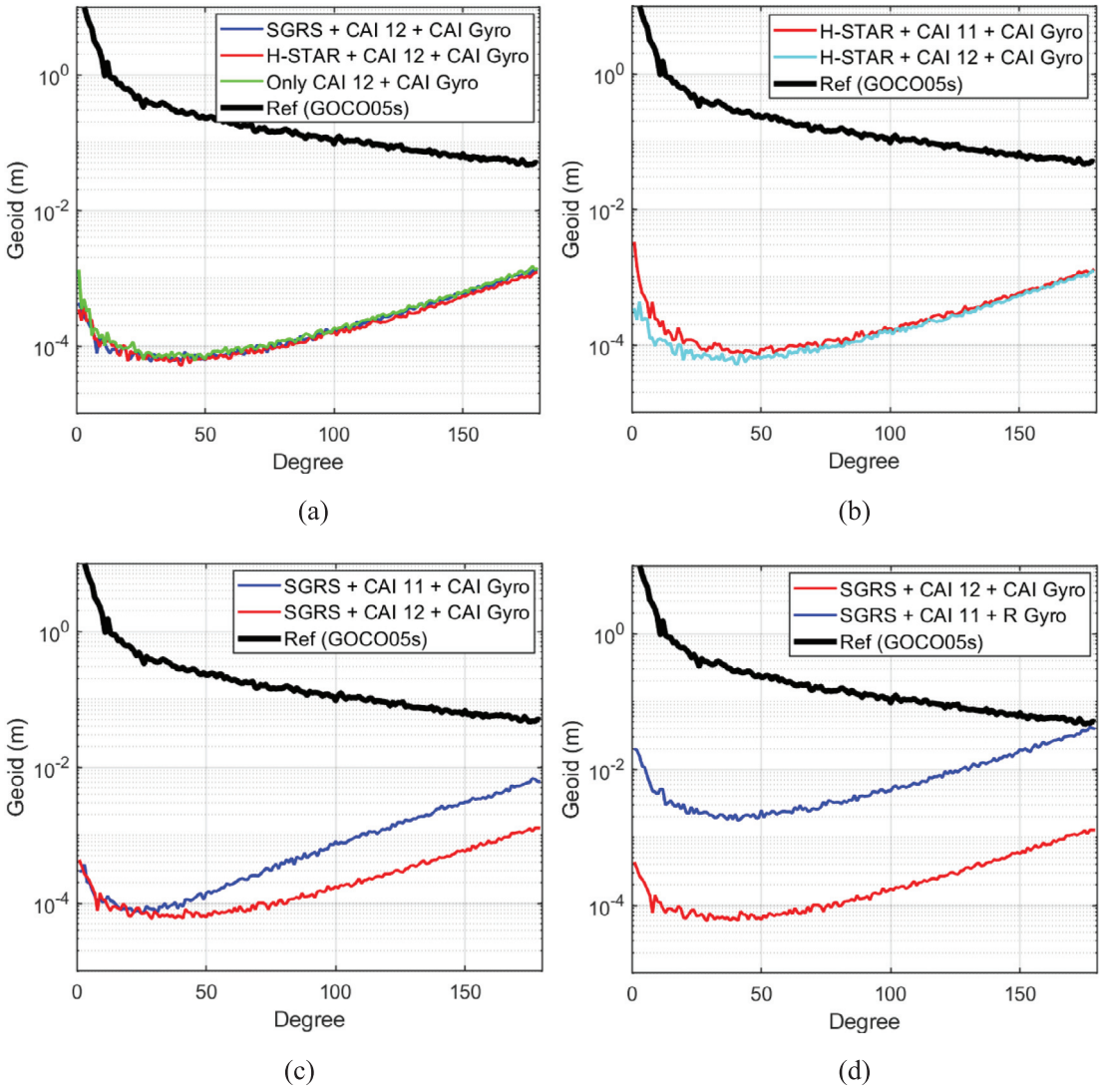


Fig. 7. The future category and their simulation in the gradiometry concept (a), the impact of the CAI ACC noise level combined with H-STAR (b), the impact of CAI ACC noise level combined with SGRS(c), and the realistic case with respect to a future case (d).

### 4.3. Future category (Future hybrid ACCs and Future Gyro)

The third group involves entirely futuristic scenarios, combining a future hybrid accelerometer with a future gyroscope. In this new hybrid ACC, EAs are combined with CAI 12, setting it apart from the previous categories. Due to the anticipated reduction in noise in the hybrid accelerometer and the use of a CAI-based gyroscope, we refer to this category as the future category. It includes: (a) SGRS + CAI 12 + CAI Gyro, (b) H-STAR + CAI 12 + CAI Gyro, and (c) CAI 12 only + CAI Gyro. Fig. 6(a) demonstrates the results for this category, showing equal behavior for all three cases. The reason for this can be understood from Fig. 3, where the a similar ASD noise for the hybrid cases is evident which closely matches CAI 12 after the hybridization process. Here, it appears that the hybridization process does not enhance the accuracy of gravity field recovery compared to using the future CAI alone.

Comparing the semi-realistic and future categories, shows that the future CAI ACC influences the hybrid accelerometers. Fig. 7(b) shows how the CAI ACC impacts the hybrid accelerometer when combined with H-STAR. This effect is noticeable at lower degree/order. The reason can be understood by comparison of Figs. 2(a) and 3(a). The ASD of hybrid accelerometers is similar in the high-frequency part but differs in the low-frequency part. This leads to a bigger improvement in the case of "H-STAR + CAI 12 + CAI Gyro" at lower degree/order, followed by similar results at higher degree/order.

Fig. 7(c) shows results when using the SGRS as EA in hybrid accelerometers. Unlike the previous case, the improvement occurs at higher degree/order. The explanation can be found by comparing of Figs. 2(b) and 3(b).

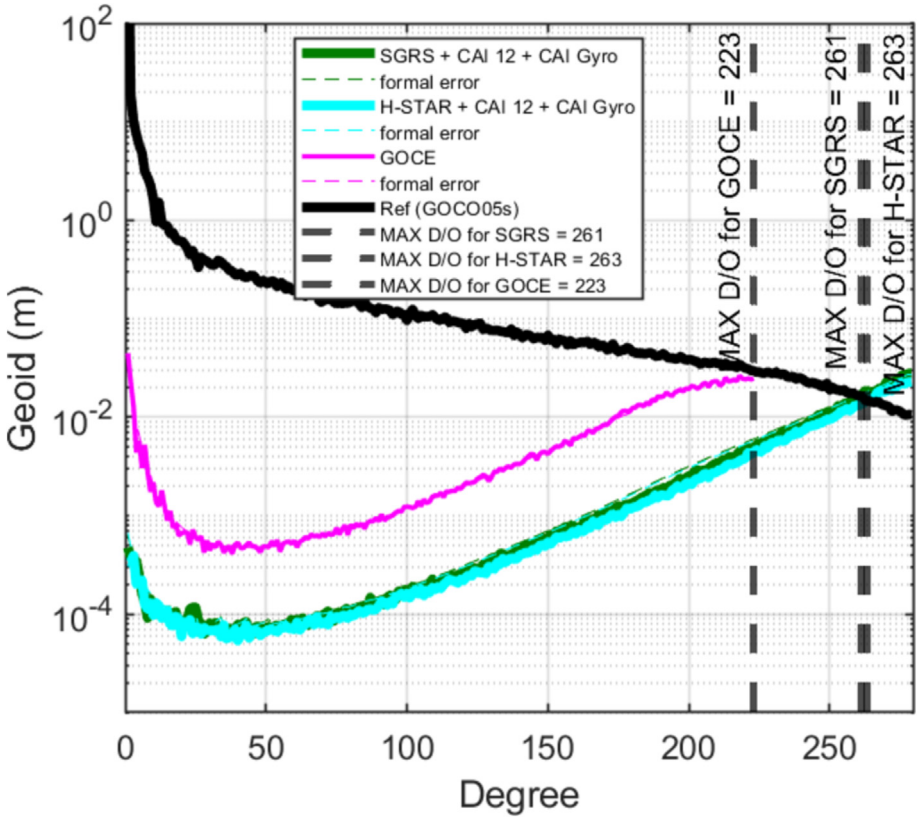


Fig. 8. Recoverable maximum degree/order, using new instruments in gradiometry – The curves of the formal errors are very similar to the true error curves and thus hidden behind them.

The main difference in the ASD of the hybrid cases is in the high-frequency part, leading to the improvement in the "SGRS + CAI 12 + CAI Gyro" case.

To better understand the impact of having an accurate CAI ACC and gyroscope, we compare a case from the realistic category with its counterpart from the future category. Fig. 7(d) illustrates this comparison, showing at least a two-order improvement between the realistic and future categories. This improvement is a result of both the impact of CAI 12 and the CAI Gyro.

### 4.4. Recovery and cumulative error

Determining the maximum resolvable degree/order in a satellite gravimetry mission is crucial for addressing static gravity field determination. We computed the resolvable maximum degree/order from a future category because its performance, and compare it with GOCE (Fig. 8). The recoverable static gravity field, can be obtained up to degree/order 263 using simulated data and system equations until D/O 280 in three months. In this section, we adjusted the maximum D/O alongside the time span of the simulation data to account for the maximum recoverable D/O. The GOCE-like setup consists of six 3D electrostatic accelerometers, each with an error level approximately five times lower (i.e., more precise) than the original design (see Touboul et al., 2016).

A good way to compare different cases is via the cumulative error in terms of the geoid. Fig. 9 shows this comparison between the different cases in each category.

In the realistic category, the cumulative error for the hybrid cases is better than GOCE up to a degree/order of 125, but after that, GOCE performs better. This indicates that hybrid accelerometers without accurate attitude observation are not useful in the gradiometry concept. However, when an accurate gyroscope is added to the hybrid accelerometers, the results change entirely, as shown in the graph for the semi-realistic category. All three cases in this category perform better than GOCE. When we compare the different cases in this category, it becomes clear how the adding of EA (SGRS and H-STAR) to hybrid accelerometers impacts the cumulative geoid error. The worst case is "CAI 11 only + CAI Gyro," i.e. without the contribution of an EA. However, the cumulative error decreases when an EA is included forming hybrid accelerometers. The case "H-STAR + CAI 11 + CAI Gyro" is better than "SGRS + CAI 11 + CAI Gyro" at higher degree/order. The reason for this is that H-STAR performs better than SGRS, especially considering the capacitive sensing of SGRS EA. When we use SGRS as EA in hybrid accelerometers, we have a lower cumulative error in determining the geoid at lower degree/order. This is because SGRS EAs perform better than H-STAR in the low-frequency part.

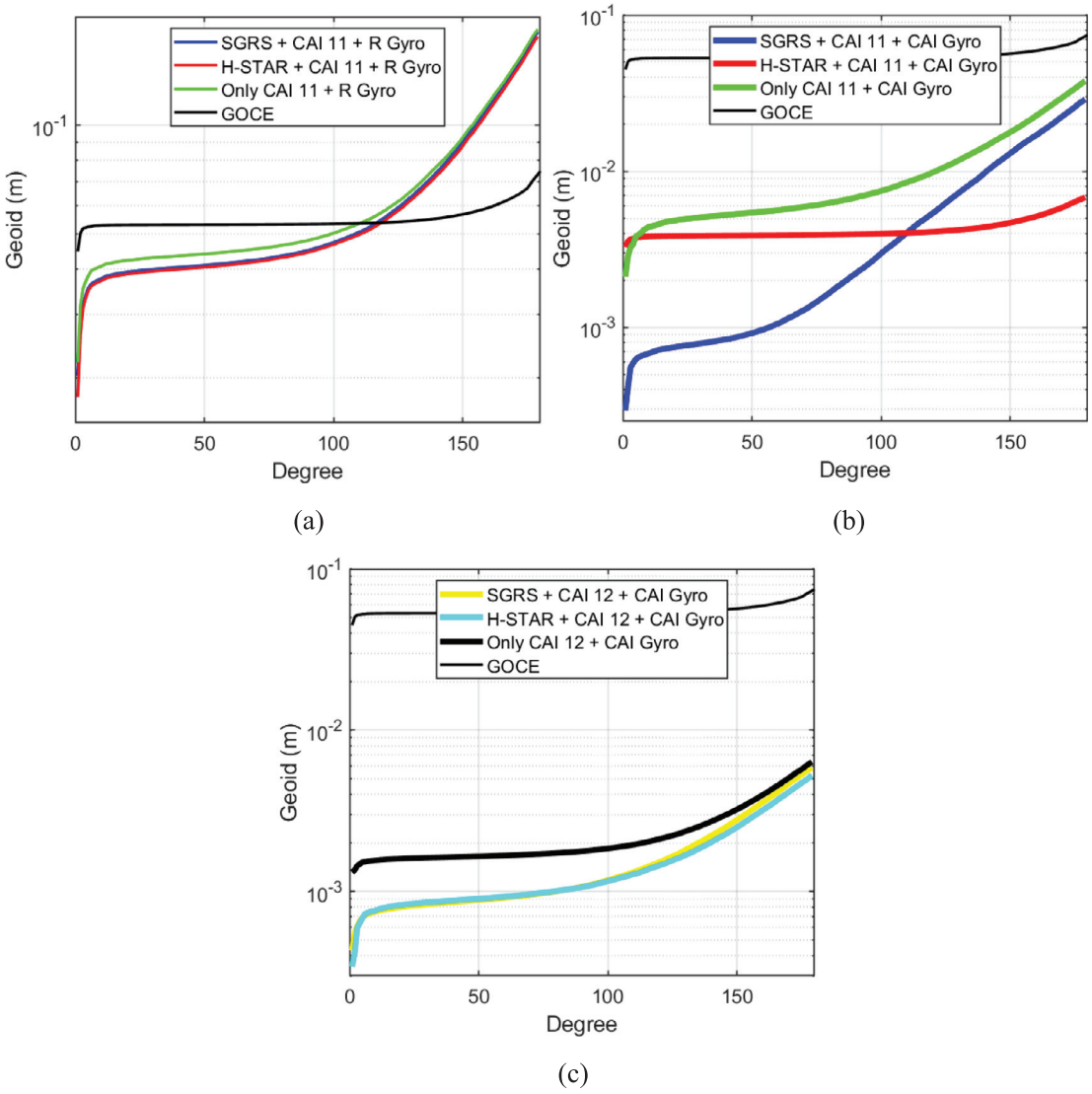


Fig. 9. Cumulative geoid error for realistic (a), semi-realistic (b) and future (c) categories compared to GOCE.

The biggest improvement is obtained in the third category and future cases. The influence of EAs is evident in the recovery results, and all three cases in this category appear similar. However, the key difference is caused by including EAs or not.

### 4.5. Time-variable gravity field

Furthermore, we investigated the potential for capturing time-variable gravity signals using the future satellite gradiometry concept. The studied scenarios from future category are: (a) H-STAR + CAI 12 + CAI Gyro, (b) SGRS + CAI 12 + CAI Gyro, (c) only CAI 12 + CAI Gyro, and (d) H-STAR + CAI 12. The inclusion of the last scenario, excluding any gyroscope noise, aims to demonstrate the specific impact of the gyroscope accuracy on determining temporal variations. Fig. 10 displays the corresponding simulation results with comparison to the monthly AOHIS model. A comparison between the cases "H-STAR + CAI 12 + CAI Gyro" and "H-STAR + CAI 12" highlights the significant influence of the gyroscope noise. Without gyroscope noise, temporal variations can be observed up to degree/order 35. However, the presence of gyroscope noise makes the retrieval of time-variable gravity signals nearly impossible. To facilitate a comparison between the SST and gradiometry concepts, a solution based on simulated GFO data (Zingerle et al., 2024) has been added to the graph.

## 5. Conclusions

In this study, we explored the potential impact of quantum accelerometers on the future satellite gravity gradiometry (SGG) mission concept. Closed-loop simulations were run to quantify the advantages of advanced instruments, specifically hybrid accelerometers and subsequently gradiometers, in comparison to classical electrostatic sensors. The results suggest that enhanced accelerometers/gra-

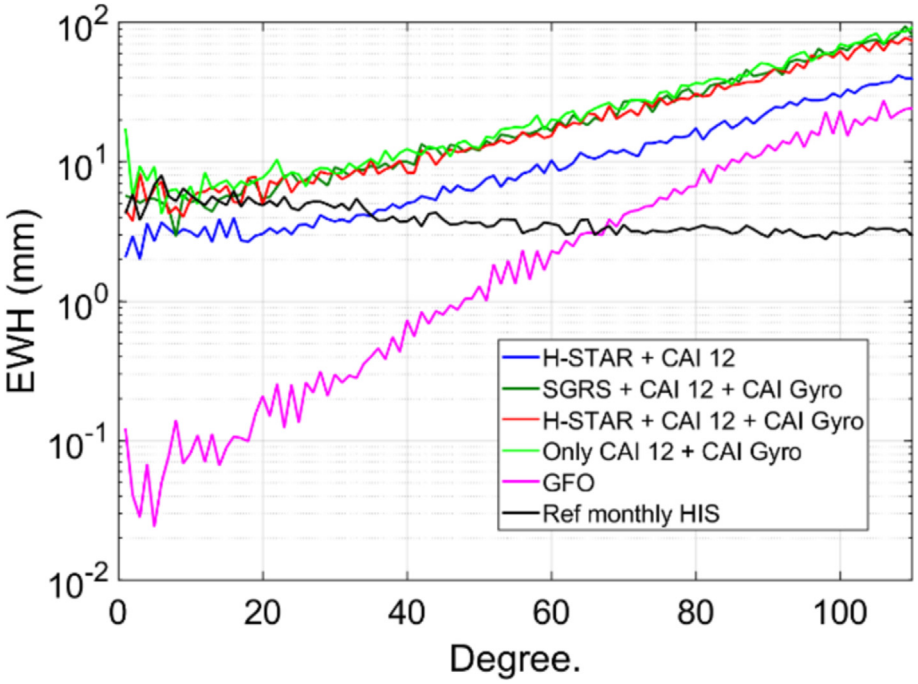


Fig. 10. Retrieved of time-variable gravity signals in terms of equivalent water height (EWH).

diometers can improve the determination of the gravity gradient compared to the GOCE mission. However, due to operational constraints of CAI ACC, one may only have one sensitive axis. Accurate knowledge of the satellite's attitude would necessitate the use of additional instruments, such as a precise gyroscope. Currently, the available attitude sensors are not sensitive enough to take full advantage of the potential improvements of future gradiometers. We assumed the future gyroscope (CAI gyroscope) as a new instrument to measure attitude data. Even with this, the expected sensitivity of future (CAI) gradiometers is not high enough to outperform SST missions in recovering the time-variable part of Earth's gravity field. Nevertheless, CAI SGG instruments have lower noise than the GOCE gradiometer, potentially allowing to determine a more accurate high-resolution static gravity field.

## Declaration of competing interest

The authors declare that they have no known competing financial interests or personal relationships that could have appeared to influence the work reported in this paper.

## Acknowledgements

The investigations were supported by funding of the German Federal Ministry of Economic Affairs and Energy (BMWi), projects 50EE2220 A/B/C (QUANTGRAV), Deutsche Forschungsgemeinschaft (DFG) –TerraQ (Project-ID 434617780 – SFB 1464), German Aerospace Center (DLR) – Q-BAGS (Project-ID 50WM2181) and Germany's Excellence Strategy – EXC-2123 "QuantumFrontiers" – 390837967. Computations were carried out using resources of the cluster system at the Leibniz University of Hannover, funded by the Deutsche Forschungsgemeinschaft (DFG) – INST 187/742-1 FUGG.

## References

Abrykosov, P., Pail, R., Gruber, T., Zahzam, N., Bresson, A., Hardy, É., Christophe, B., Bidel, Y., Carraz, O., Siemes, C., 2019. Impact of a novel hybrid accelerometer on satellite gravimetry performance. *Adv. Space Res.* 63 (10), 3235–3248. https://doi.org/10.1016/j.asr.2019.01.034.

Antoine, C., Bordé, C.J., 2003. Quantum theory of atomic clocks and gravito-inertial sensors: An update. *J. Opt. B Quantum Semiclassical Opt.* 5 (2), S199–S207. https://doi.org/10.1088/1464-4266/5/2/380.

Armano, M., Audley, H., Baird, J., Binetruy, P., Born, M., Bortoluzzi, D., Castelli, E., Cavalleri, A., Cesarini, A., Cruise, A.M., Danzmann, K., de Deus Silva, M., Diepholz, I., Dixon, G., Dolesi, R., Ferraioli, L., Ferroni, V., Fitzsimons, E.D., Freschi, M., Gesa, L., Gibert, F., Giardini, D., Giusteri, R., Grimani, C., Grzymisch, J., Harrison, I., Heinzel, G., Hewitson, M., Hollington, D., Hoyland, D., Hueller, M., Inchauspé, H., Jennrich, O., Jetzer, P., Karnesis, N., Kaune, B., Korsakova, N., Killow, C.J., Lobo, J.A., Lloro, I., Liu, L., López-Zaragoza, J.P., Maarschalkerweerd, R., Mance, D., Meshksar, N., Martín, V., Martin-Polo, L., Martino, J., Martin-Porqueras, F., Mateos, I., McNamara, P.W., Mendes, J., Mendes, L., Nofrarias, M., Paczkowski, S., Perreur-Lloyd, M., Petiteau, A., Pivato, P., Plagnol, E., Ramos-Castro, J., Reiche, J., Robertson, D.I., Rivas, F., Russano, G., Slutsky, J., Sopuerta, C.F., Sumner, T., Texier, D., Thorpe, J.I., Vetrugno, D., Vitale, S., Wanner, G., Ward, H., Wass, P.J., Weber, W. J., Wissel, L., Wittchen, A., Zweifel, P., 2018. Beyond the required LISA free-fall performance: New LISA Pathfinder results down to 20 μHz. *Phys. Rev. Lett.* 120 (6). https://doi.org/10.1103/PhysRevLett.120.061101 061101.

Christophe, B., Boulanger, D., Foulon, B., Huynh, P., Lebat, V., Liorzou, F., Perrot, E., 2015. A new generation of ultra-sensitive electrostatic

accelerometers for GRACE Follow-on and towards the next generation gravity missions. *Acta Astron.* 117, 1–7. https://doi.org/10.1016/j.actaastro.2015.06.021.

Dalin, M., Lebat, V., Boulanger, D., Liorzou, F., Christophe, B., Rodrigues, M., Huynh, P., 2020. ONERA accelerometers for future Gravity Mission. *EGU* 2020. https://doi.org/10.5194/egusphere-egu2020-5721.

Dávila Álvarez, A., Knudtson, A., Patel, U., Gleason, J., Hollis, H., Sanjuán, J., Doughty, N., McDaniel, G., Lee, J., Leitch, J., Bennett, S., Bevilacqua, R., Mueller, G., Spero, R., Ware, B., Wass, P., Wiese, D. N., Ziemer, J., Conklin, J., 2022. A simplified gravitational reference sensor for satellite geodesy. *J. Geod.* 96 (10). https://doi.org/10.1007/s00190-022-01659-0.

Dobslaw, H., Bergmann-Wolf, I., Dill, R., Forootan, E., Klemann, V., Kusche, J., Sasgen, I., 2015. The updated ESA Earth System Model for future gravity mission simulation studies. *J. Geod.* 89 (5), 505–513. https://doi.org/10.1007/s00190-014-0787-8.

Dolesi, R., Bortoluzzi, D., Bosetti, P., Carbone, L., Cavalleri, A., Cristofolini, I., Da Lio, M., Fontana, G., Fontanari, V., Foulon, B., Hoyle, C.D., Hueller, M., Nappo, F., Sarra, P., Shaul, D., Sumner, T. J., Weber, W.J., Vitale, S., 2003. Gravitational sensor for LISA and its technology demonstration mission. *Class. Quantum Gravity* 20 (10), S99–S108. https://doi.org/10.1088/0264-9381/20/10/312.

Douch, K., Wu, H., Schubert, C., Müller, J., Pereira dos Santos, F., 2018. Simulation-based evaluation of a cold atom interferometry gradiometer concept for gravity field recovery. *Adv. Space Res.* 61 (5), 1307–1323. https://doi.org/10.1016/j.asr.2017.12.005.

Drinkwater, M.R., Floberghagen, R., Haagmans, R., Muzi, D., Popescu, A., 2003. GOCE: ESA's first Earth Explorer core mission. In: *Space Sciences Series of ISSI*, pp. 419–432. https://doi.org/10.1007/978-94-017-1333-7_36.

Flechtner, F., Webb, F., Watkins, M., 2017. Current status of the GRACE follow-on mission. Geophys. Res. Abstr. 19, EGU 2017–4566, EGU General Assembly 2017.

HosseiniArani, A., Schilling, M., Beaufils, Q., Knabe, A., Tennstedt, B., Kupriyanov, A., Schön, S., Pereira dos Santos, F., Müller, J., 2024. Advances in atom interferometry and their impacts on the performance of quantum accelerometers on-board future satellite gravity missions. *Adv. Space Res.* 74 (7), 3186–3200. https://doi.org/10.1016/j.asr.2024.06.055.

Josselin, V., Touboul, P., Kielbasa, R., 1999. Capacitive detection scheme for space accelerometers applications. *Sens. Actuators, A* 78 (2–3), 92–98. https://doi.org/10.1016/S0924-4247(99)00227-7.

. The Benefit of Accelerometers Based on Cold Atom Interferometry for Future Satellite Gravity Missions vol. 154, 213–220. https://doi.org/10.1007/1345_2022_151.

Kornfeld, R.P., Arnold, B.W., Groß, M., Dahya, N., Klipstein, W., Gath, P., Bettadpur, S., 2019. GRACE-FO: The gravity recovery and climate experiment follow-on mission. *J. Spacecr. Rocket.* 56 (3), 931–951. https://doi.org/10.2514/1.a34326.

Kupriyanov, A., Reis, A., Schilling, M., Müller, V., Müller, J., 2024. Benefit of enhanced electrostatic and optical accelerometry for future gravimetry missions. *Adv. Space Res.* 73 (6), 3345–3362. https://doi.org/10.1016/j.asr.2023.12.067.

Lévèque, T., Fallet, C., Lefebve, J., Piquereau, A., Gauguet, A., Battelier, B., Bouyer, P., Gaaloul, N., Lachmann, M., Piest, B., Rasel, E.M., Müller, J., Schubert, C., Beaufils, Q., Pereira dos Santos, F., 2022. CARIOQA: Definition of a Quantum Pathfinder Mission. In: Minoglou, Kyriaki, Karafolas, Nikos, Cugny, Bruno (Eds.), International Conference on Space Optics — ICSO 2022. International Conference on Space Optics — ICSO 2022. Dubrovnik, Croatia, 10/3/2022–10/7/2022. https://doi.org/10.1117/12.2690536.

Meister, J., Bremer, S., HosseiniArani, A., Leipner, A., List, M., Müller, J., Schilling, M., 2022. Reference Mirror Misalignment of Cold Atom Interferometers on Satellite-Based Gravimetry Missions. 73rd International Astronautical Congress (IAC), Proceedings.

Migliaccio, F., Reguzzoni, M., Rosi, G., Braitenberg, C., Tino, G.M., Sorrentino, F., Mottini, S., Rossi, L., Koç, Ö., Batsukh, K., Pivetta, T., Pastorutti, A., Zoffoli, S., 2023. The MOCAST+ study on a quantum gradiometry satellite mission with atomic clocks. *Surv. Geophys.* 44 (3), 665–703. https://doi.org/10.1007/s10712-022-09760-x.

Müller, J., Wu, H., 2020. Using quantum optical sensors for determining the Earth's gravity field from space. *J. Geod.* 94 (8). https://doi.org/10.1007/s00190-020-01401-8.

Pereira dos Santos, F., Landragin, A., 2007. Getting the measure of atom interferometry. *Phys. World* 20 (11), 32–37. https://doi.org/10.1088/2058-7058/20/11/38.

Purkhauser, A., Pail, R., 2020. Triple-Pair constellation configurations for temporal gravity field retrieval. *Remote Sens. (Basel)* 12 (5), 831. https://doi.org/10.3390/rs12050831.

Roth, M., Baur, O., Keller, W., 2012. "Brute-Force" solution of Large-Scale systems of Equations in a MPI-PBLAS-ScaLAPACK environment. In: Springer eBooks, pp. 581–594. https://doi.org/10.1007/978-3-642-23869-7_42.

Savoie, D., Altorio, M., Fang, B., Sidorenkov, L.A., Geiger, R., Landragin, A., 2018. Interleaved atom interferometry for high-sensitivity inertial measurements. *Sci. Adv.* 4 (12). https://doi.org/10.1126/sciadv.aau7948.

Schilling, M., Müller, J., Timmen, L., 2012. Einsatz der Atominterferometrie in der Geodäsie. *Zfv* 137, 185–194. https://doi.org/10.15488/3097.

Siemes, C., 2018. Improving GOCE cross-track gravity gradients. *J. Geod.* 92 (1), 33–45. https://doi.org/10.1007/s00190-017-1042-x.

Stummer, C., Fecher, T., Pail, R., 2011. Alternative method for angular rate determination within the GOCE gradiometer processing. *J. Geod.* 85 (9), 585–596. https://doi.org/10.1007/s00190-011-0461-3.

Tapley, B.D., Bettadpur, S., Watkins, M.M., Reigber, C., 2004. The gravity recovery and climate experiment: Mission overview and early results. *Geophys. Res. Lett.* 31 (9). https://doi.org/10.1029/2004gl019920.

Torge, W., Müller, J., Pail, R., 2023. Geodesy, 5th Edition. De Gruyter. https://doi.org/10.1515/9783110250008.

Touboul, P., Métris, G., Selig, H., Traon, O.L., Bresson, A., Zahzam, N., Christophe, B., Rodrigues, M., 2016. Gravitation and geodesy with inertial sensors, from ground to space. *AerospaceLab* 12, 11. https://doi.org/10.12762/2016.al12-11.

Zahzam, N., Christophe, B., Lebat, V., Hardy, É., Huynh, P., Marquet, N., Blanchard, C., Bidel, Y., Bresson, A., Abrykosov, P., Gruber, T., Pail, R., Daras, I., Carraz, O., 2022. Hybrid electrostatic–atomic accelerometer for future space gravity missions. *Remote Sens. (Basel)* 14 (14), 3273. https://doi.org/10.3390/rs14143273.

Zingerle, P., Romeshkani, M., Haas, J., Gruber, T., Güntner, A., Müller, J., Pail, R., 2024. The benefits of future quantum accelerometers for satellite gravimetry. *Earth Space Sci.* 11 (9). https://doi.org/10.1029/2024EA003630 e2024EA003630.

Zund, J.D., 1994. Algebraic theory of the Marussi tensor. In: Springer eBooks, pp. 255–271. https://doi.org/10.1007/978-3-642-79187-1_8.